SPACECRAFT POTENTIAL INFLUENCED BY METEOROID HYPERVELOCITY IMPACTS

Jakub Vaverka[1], Asta Pellinen-Wannberg[1,2], Johan Kero[2], Ingrid Mann[1,3], Alexandre De Spiegeleer[1], Maria Hamrin[1], Carol Norberg[1], and Timo Pitkänen[1]

[1]*Department of Physics, Umeå University, Sweden.*
[2]*Swedish Institute of Space Physics, Kiruna, Sweden.*
[3]*EISCAT Scientific Association, Kiruna, Sweden.*

ABSTRACT

Dust impacts on the spacecraft body in various plasma environments lead to different responses in the spacecraft potential. This fact complicates dust detection by Earth orbiting spacecraft crossing various parts of the Earth magnetosphere. Theoretical studies of dust impacts under a selection of plasma conditions can be a very useful tool for understanding the data measured by spacecraft in various environments. We present a numerical simulation of spacecraft charging including currents generated by dust impacts for various plasma environments to show the influence of the plasma parameters to dust impact detection by monopole electric field instruments.

1. INTRODUCTION

A plasma cloud generated by a hypervelocity dust impact on a spacecraft body can be detected by the electric field instruments as change of the potential of the spacecraft or the electric antenna [1]. These instruments offer a complementary method to the conventional dust detectors in situ. There are electric field instruments on the majority of spacecraft. Since Earth-orbiting missions are generally not equipped with conventional dust detectors employing electric field instruments offers a unique chance to monitor the Earth's dust environment. Another advantage of the method is that the entire spacecraft surface is used as the collection area providing flux data with better statistics. The interplanetary missions Voyager [2], Deep Space 1 [3], Cassini [4, 5], Wind [6, 7], and STEREO [8, 1, 9] have successfully used this method for dust detection. The sensitivity of the wave instruments strongly depends on their design and the topography of antennas. Generally monopole detectors are much more sensitive to dust impacts than dipole antennas.

2. SPACECRAFT CHARGING

A spacecraft body immersed in a plasma environment is charged mainly by photoemission and collection of electrons and ions. The equilibrium potential is set by balance of all charging currents and depends on the ambient plasma environment, solar UV irradiation and composition of the spacecraft surface. The typical spacecraft potential is slightly positive in the case when the spacecraft body is illuminated by solar UV radiation.

The spacecraft potential can be influenced by hypervelocity dust impacts on the spacecraft body for a short time. The dust impact generates a plasma cloud by impact ionization. The recollection of electrons by the positively charged spacecraft body causes a change in the spacecraft potential followed by relaxation to the equilibrium value. The relaxation time strongly depends on the ambient plasma environment. The recollection of plasma cloud particles can influence not only the spacecraft potential but also the potential of antennas for measuring of the electric field [1].

The evolution of the spacecraft potential Φ_{SC} is described by the current balance equation with the main charging currents being photoemission, J_{pho} and collection of electrons, J_e and ions, J_i:

$$\frac{dQ_{SC}}{dt} = \frac{d(C\Phi_{SC})}{dt} = J = J_{pho} + J_e + J_i + J_{sec}. \quad (1)$$

where Q_{SC} is the spacecraft charge and C is the spacecraft capacitance calculated for a sphere of radius, r = 1 m (Cluster like spacecraft). The secondary electron emission current, J_{sec} can be important in environments where the electron temperature is higher than 10 eV.

We use the assumption of a spherical spacecraft of radius, r = 1 m immersed in a collisionless Maxwellian plasma described by electron and ion temperatures T_e and T_i and densities n_e and n_i. The Orbital Motion Limited (OML) theory is used to calculate the ion and electron

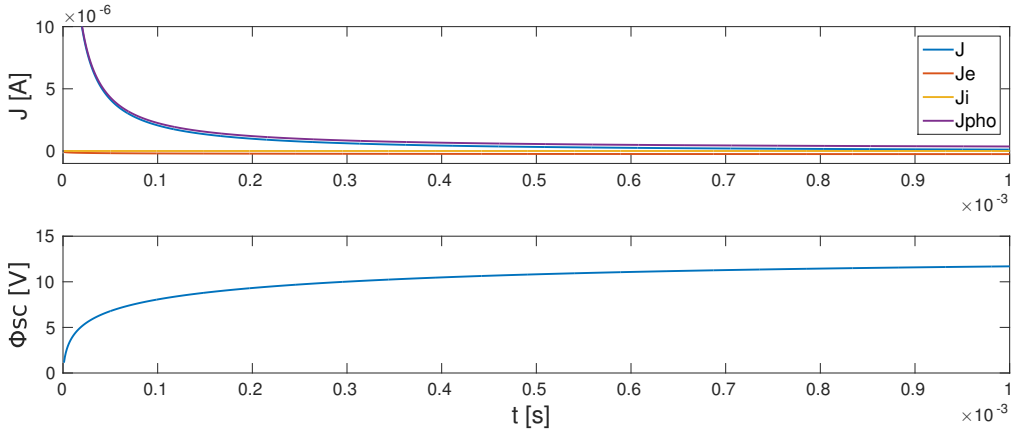

Figure 1. The temporal evolution of all charging currents (top) and the spacecraft potential (bottom) for density of electrons and ions $n = n_e = n_i = 0.1$ cm^{-3} and plasma temperature $T = T_e = T_i = 5$ eV

currents [10, 11, 12, 13]. This results in the following expression for the electron current:

$$J_e = J_{0e} \times \begin{cases} \exp(+e\Phi_{SC}/k_B T_e) & \Phi_{SC} < 0 \\ (1 + e\Phi_{SC}/k_B T_e) & \Phi_{SC} \geq 0, \end{cases} \quad (2)$$

where k_B is the Boltzmann constant, e is the elementary charge, and $J_{0e} = 4\pi r^2 e n_e (k_B T_e / 2\pi m_e)^{1/2}$.

Similarly, the ion current:

$$J_i = J_{0i} \times \begin{cases} \exp(-e\Phi_{SC}/k_B T_i) & \Phi_{SC} \geq 0 \\ (1 - e\Phi_{SC}/k_B T_i) & \Phi_{SC} < 0. \end{cases} \quad (3)$$

The current of photoelectrons from a conductive surface at 1 AU for a Maxwellian energy distribution of photoelectrons is given by known formula [10, 13]:

$$J_{pho} = J_{pho0} \times \begin{cases} 1 & \Phi_{SC} < 0 \\ \exp(-e\Phi_{SC}/k_B T_{pho}) & \Phi_{SC} \geq 0, \end{cases} \quad (4)$$

where T_{pho} is the temperature of photoelectrons and $J_{pho0} = 2.5 \times 10^{14} \pi r^2 e$.

We used the Sternglass formula [14, 12] for the yield of the secondary electron emission and use the same approach as Horanyi [12] for the calculation of the secondary emission current. It is important to note that backscattered electrons are not included in this approach and it is necessary to calculate their contribution separately. We use a simple model where backscattered electrons are included only when the temperature of electrons is higher than 20 eV with a constant yield of 20 %.

The recollection current of charged particles from the plasma cloud generated by the dust impact, J_{rec} can be described by the Gaussiann function [1]. The time constant for the recollection (Gaussian function) measured by the STEREO spacecraft in the solar wind is approximately 30 μs [1]. We use this value in the simulation. The amount of charge recollected by the spacecraft body strongly depends on the velocity and the mass of impacting grains [1, 15]. It is possible to derive combinations of the velocity and the mass of the impacting dust grain from the amplitude of the pulse in the spacecraft potential.

3. RESULTS AND DISCUSSION

We use a numerical model for calculation of the spacecraft potential under various plasma environment conditions starting from Eq. 1. The simulation starts with an uncharged spacecraft and time step 1 μs. The photoemission (due to the solar UV radiation) with the temperature of photoelectrons T_{pho} = 2 eV is included in all simulations. The secondary electron emission strongly depends on the composition of the spacecraft surface. We use parameters δ_m = 1 and E_m = 300 eV for the Sternglas formula representing the conductive surface of the spacecraft [14, 12].

The temporal evolution of all charging currents (top) and the spacecraft potential (bottom) for the density of electrons and ions $n = n_e = n_i = 0.1$ cm^{-3} and plasma temperature $T = T_e = T_i = 5$ eV are shown in Fig. 1. The secondary electron emission is not included in this case because of the low energy of the electrons. It is possible to see that the spacecraft reached the equilibrium potential (12.4 V) in approximately 1 ms. The photoemission is the dominant charging process when the potential of the spacecraft is low (first 200 μs of the simulation) and balanced by the electron current at the equilibrium potential.

The current caused by the dust impact is added to the simulation when the spacecraft potential is at the equilibrium value. The simulation step is reduced to 10 ns in this case. The total charge recollected by the spacecraft body in the simulation is $Q = 10^{-10}$ C correspond-

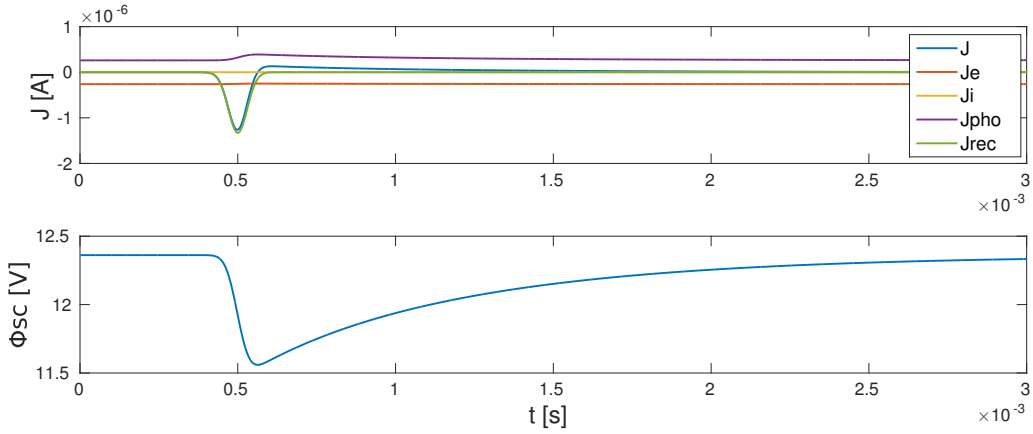

Figure 2. The temporal evolution of all charging currents (top) and the spacecraft potential (bottom) after dust impact.

ing to a grain of radius 1 μm impacting with the velocity 20 km/s. The temporal evolution of all charging currents (top) and the spacecraft potential (bottom) after the dust impact are shown in Fig. 2. It is possible to see that the dust impact caused a drop in the spacecraft potential from the equilibrium value (12.4 V) to approximately 11.5 V and the consequent relaxation to the equilibrium state takes approximately 3 ms. This pulse can be detected by monopole electric field instruments using the potential of the spacecraft body as one reference for measuring the electric field.

Similar simulations for sets of various plasma conditions (density of electrons and ions $n = n_e = n_i = 0.1$ and 1 cm^{-3} and plasma temperature $T = T_e = T_i = 5$ and 300 eV) are shown in Fig 3. the top panel shows the spacecraft potential and the bottom panel shows the change in the equilibrium potential influenced by the dust impact for different plasma environments. It is possible to see that the equilibrium spacecraft potential, amplitude of pulse generated by the dust impact and relaxation time strongly depend on the ambient plasma environment. The crucial parameter is the electron density. The spacecraft potential is more sensitive to dust impacts when the plasma density is low (higher spacecraft potential). Currents of photoelectrons and electrons at equilibrium are large enough that the current generated by a dust impact (J_{rec}) causes only small and short change in the spacecraft potential in the case of high electron density (10 cm^{-3}).

The simple model of spacecraft charging shows (Fig. 3.) that the dust impact causes different responses in the spacecraft potential in various plasma environments. This fact is important when changes in the spacecraft potential are used for detection of dust impacts on the spacecraft body by the Earth-orbiting spacecraft crossing different regions of the magnetosphere. The very important result is that the sensitivity of such instruments for the dust detection change significantly during the spacecraft orbit.

Other parameters influencing the spacecraft potential are distributions of photoelectrons and secondary electrons and the yield of the secondary electron emission (composition of the spacecraft surface). Some of the spacecraft are equipped with an active potential control to limit the high positive potential. The detailed simulation of the influence of dust impacts on the spacecraft potential for various parts of the Earth's magnetosphere including factors mentioned above and comparison with detected pulses by the Cluster spacecraft will be described in the special issue of IEEE TPS.

ACKNOWLEDGMENTS

This work was supported by the Swedish National Space Board (SNSB).

REFERENCES

[1] Zaslavsky, A. (2015), Floating potential perturbations due to micrometeoroid impacts: Theory and application to S/WAVES data, *J. Geophys. Res. Space Physics*, *120*(2), 855–867.

[2] Gurnett, D. A., Grn, E., Gallagher, D., Kurth, W. S., and Scarf,F. L. (1983), Micron-sized particles detected near Saturn by the Voyager plasma wave instrument, *Icarus*, *53*(2), 236–254.

[3] Tsurutani, B.T., Clay, D.R., Zhang, L.D., Dasgupta, B., Brinza, D., Henry, M., Arballo, J.K., Moses, S., and Mendis, A. (2004), Plasma clouds associated with Comet P/Borrelly dust impacts, *Icarus*, *167*(1), 89–99.

[4] Wang, Z., Gurnett, D. A., Averkamp, T. F., Persoon, A. M., and Kurth, W. S. (2006), Characteristics of dust particles detected near Saturn's ring plane with the Cassini Radio and Plasma Wave instrument, *Planet. Space Sci.*, *54*(9-10), 957–966.

[5] Kurth, W. S., Averkamp, T. F., Gurnett, D. A., and Wang,Z. (2006), Cassini RPWS observations of dust in Saturn's E Ring, *Planet. Space Sci.*, *54*(9-10), 988–998.

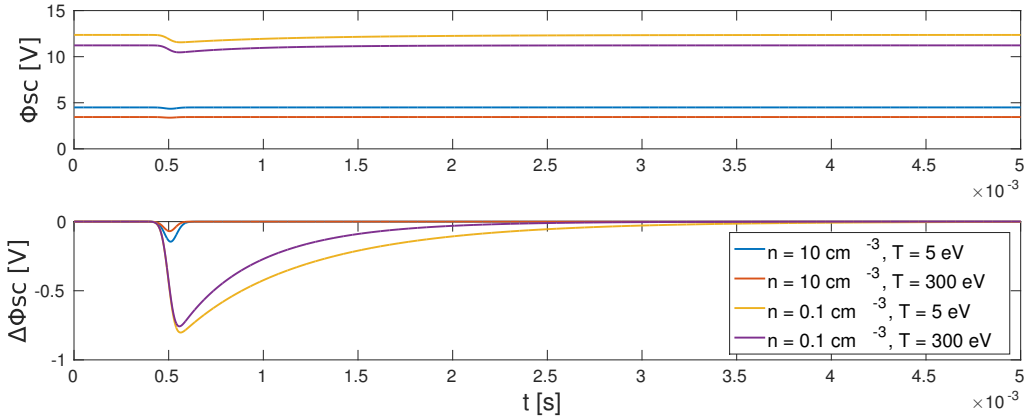

Figure 3. The temporal evolution of the spacecraft potential (top) and change in the equilibrium potential (bottom) during dust impact for various plasma environments.

[6] Malaspina, D. M., Horanyi, M., Zaslavsky, A., Goetz, K., Wilson, L. B., and Kersten, K. (2014), Interplanetary and interstellar dust observed by the Wind/WAVES electric field instrument, *Geophys. Res. Lett.*, *41*(2), 266–272.

[7] Wood, S. R., Malaspina, D. M., Andersson, L., and Horanyi, M. (2015), Hypervelocity dust impacts on the Wind spacecraft: Correlations between Ulysses and Wind interstellar dust detections, *J. Geophys. Res. Space Physics*, *120*(9), 7121–7129.

[8] Zaslavsky, A., Meyer-Vernet, N., Mann, I., Czechowski, A., Issautier, K., Le Chat, G., Pantellini, F., Goetz, K., Maksimovic, M., Bale, S. D., and Kasper, J. C. (2012), Interplanetary dust detection by radio antennas: Mass calibration and fluxes measured by STEREO/WAVES, *J. Geophys. Res. Space Physics*, *117*(5).

[9] Malaspina, D. M., O'Brien, L. E., Thayer, F., Sternovsky, Z., and Collette, A. (2015), Revisiting STEREO interplanetary and interstellar dust flux and mass estimates, *J. Geophys. Res. Space Physics*, *120*(8), 6085–6100.

[10] Whipple, E. C. (1981), Potentials of surfaces in space, *Rep. Prog. Phys.*, *44*(11), 1197–1250.

[11] Meyer-Vernet, N. (1982), "Flip-flop" of electric potential of dust grain in space, *Astron. Astrophys.*, *105*(1), 98–106.

[12] Horanyi, M. (1996), Charged dust dynamics in the solar system, *Annu. Rev. Astron. Astrophys.*, *34*, 383–418.

[13] Vaverka, J., I. Richterova, J. Pavlu, J. Safrankova, and Z. Nemecek (2013), Numerical calculation of an equilibrium dust grain potential in lunar environment, *IEEE Trans. Plasma Sci.*, *41*(4), 740–744.

[14] Sternglass, E. (1957), *Theory of Secondary Electron Emission Under Electron Bombardement*, Westinghause Research Laboratories.

[15] Collette,A. and Grün,E. and Malaspina, D. and Sternovsky,Z. (2014), Micrometeoroid impact charge yield for common spacecraft materials, *J. Geophys. Res. Space Physics*, *119*, 6019–6026.